Finger Worn UHF Far Field RFID Tag Antenna

Paul S. Taylor and John C. Batchelor, *Senior Member, IEEE*

***Abstract*—This paper presents the design and measurement of an experimental passive UHF RFID tag worn as a ring with applications particularly in healthcare or secure environments. Three sizes of rings were designed for the European UHF RFID band over two different substrates at varying heights off the skin. Designing effective body mounted antennas for passive RFID is very challenging, particularly when mounted directly upon the skin. The rings were simulated with a commercial electromagnetic simulation software and then constructed and tested on an adult male ring finger over several angles of RF illumination so that read ranges and directivity could be determined. Main beam read distances between 2 and 5m where achieved dependent on the ring substrate height.**

***Index Terms*—Body worn antennas, healthcare monitoring, magnetic loop, radio frequency identification (RFID), security monitoring, small loop antennas, wearable sensor.**

I. Introduction

Recent advances in epidermal electronics exploit miniaturized components, low power technologies and materials science resulting in thin flexible substrates and interconnects, for user comfort and longer wear life [1]-[3]. However, the RF block power requirements of conventional wireless devices dominate the power budget.

UHF RFID has advanced into applications beyond asset tracking through the innovative use of inventory transponder chips coupled with novel antenna designs and more functional transponder chips [4]-[15]. These non-body mounted tags are passive, powered only by the reader RF power, with the backscattered signal returning data over several meters. This has led to on-body tag research for various applications, including healthcare where antenna efficiency challenges arise due to the UHF band losses of the human body which cause read ranges to reduce from over 10 m in air to 1-1.5 m for an optimized on-skin design. Greater efficiency can be obtained with isolation from the skin for patch antennas and similar structures but at the expense of increased height [16]-[17].

This paper considers small loop antennas (SLAs) or magnetic loops for use as finger mounted tags for far field reading over several meters. SLAs have circumferences < 0.1λ and are primarily used at long wavelength HF owing to their efficient performance and compact dimensions compared to resonant structures [18]-[19]. Although not normally considered for UHF - as antennas are already relatively compact – the SLA has potential as an RFID loop antenna where the size and shape is defined by the finger or toe.

Section II demonstrates the theory of SLA operation including feed arrangement on an adult male ring finger for various diameters and thicknesses of ring. Section III describes ring simulations carried out on a single finger and three finger phantom to obtain the design impedance matches, efficiencies and radiation patterns. Section IV details the practical construction and measurements of the samples to be tested with read range and directivity measurements for the three designs. The paper closes with concluding remarks that summarize the designs and measurements.

II. The Small Loop Antenna

A. Theory of Operation

A single turn circular SLA is considered small when conductor length is < 0.1λ, this results in a near uniform in-phase perimeter current. The loop behaves as a lumped inductance which can be resonated at the frequency of interest with a capacitor, forming a high-Q parallel tuned circuit. The basic components of an SLA, minus its feed are shown in Fig. 1. along with its equivalent circuit.

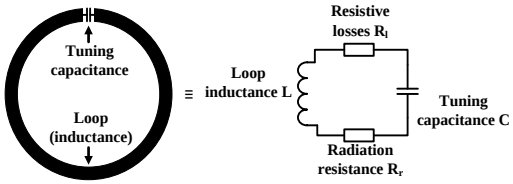

Fig. 1. Basic components of an SLA and its equivalent circuit.

The inductance of a single turn circular loop can be found by [20]:

$$L = \frac{\mu}{2} D \left[ln\left(\frac{8D}{d}\right) - 2 \right] \quad (1)$$

where: D = loop diameter
d = conductor diameter.

The value of the tuning capacitor can be found by $C_{Tune} = 1/\omega^2 L$. The radiation resistance R_r depends only on the loop area and is given in (2). This is typically a very low value, tens of mΩ for the loops discussed here. The loop also has both ohmic and skin effect losses which need to be minimized to

Manuscript received March 4, 2019; This work was supported by the U.K. Engineering and Physical Sciences Research Council project EP/P027075/1.
P.S. Taylor and J. C. Batchelor are with the School of Engineering and Digital Arts, University of Kent, Canterbury CT2 7NT, U.K. (e-mail: p.taylor-250@kent.ac.uk; j.c.batchelor@kent.ac.uk).

maximize its efficiency;

$$R_r = 320\pi^4 \left(\frac{A}{\lambda^2}\right) \Omega \quad (2)$$

where: A = the area of the loop.

The SLA is a linearly polarized antenna and must be orientated correctly for optimum performance. The far field radiation pattern of an SLA is equivalent to that of a small electric dipole normal to the loop plane.

B. Resonating Capacitor

High frequency SLAs can be used over a wide frequency range, with 3:1 being typical. This is achieved with a variable capacitor as the main tuning element but which also introduces ohmic losses [21]. RFID is narrow band, so a fixed value capacitor can be used. This could be a lumped element but there will still be losses and solder connections will be required. The solution presented here is to overlap the loop ends with a suitable dielectric to form a low loss parallel plate capacitor.

C. Input Coupling and Matching

Loop coupling or impedance tap matching can be used to couple a source to an SLA [22], and the impedance tap (gamma match) is employed here. The match consists of a section of conductor parallel to the main loop, fed diametrically opposite the tuning capacitor. The tap point to the loop perimeter is chosen to achieve an optimum match to the RFID transponder, which will typically have a low real value and a capacitive imaginary part.

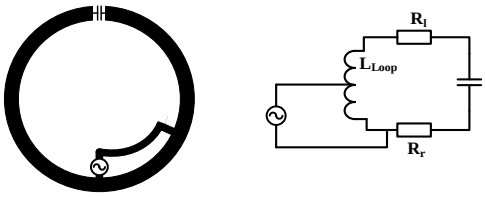

Fig. 2. Gamma match method of feeding an SLA.

III. Simulations and Results

A. Simulation Measurements

Simulations were carried out using CST MWS™, where the SLA model consisted of the main copper foil element, substrate material, lumped element tuning capacitor, source and finger phantom. This obtained reference values for the directivity, efficiency and return loss. A second phantom consisting of adjacent fingers and hand section was then modelled and simulated. The three ring samples tested had diameters of 21, 22 and 23 mm. This relates to their final dimensions when placed upon their target platform. These dimensions result in conductor circumferences of ~0.18λ, 0.19λ and 0.2λ at 866 MHz. The conductor width was arbitrarily chosen at 5 mm. It is known that wide conductors offer increased efficiency over narrow ones, while a narrow conductor will give a greater inductance for the same unit length but may not offer enough surface area at its overlap to achieve the required capacitance to resonate the loop. For example, if the required capacitance value required an area of 10 mm^2 this can be achieved with a 2 mm overlap for a 5 mm wide conductor, or for a 1 mm wide conductor an overlap of 10 mm would be required, consequently reducing the antenna effective area and hence its efficiency.

The prototype antennas were fabricated from copper foil with a thickness of 35 µm. For input coupling, the co-planar gamma match suits the ring topology presented here, where also the additional inductance offered by the gamma match can be utilized in cancelling or part-cancelling the capacitive reactance of the RFID chip. An empirical method was used to design the gamma match and achieve an efficient match to the impedance of the RFID device, which in this case is the Alien Higgs 3 with an input impedance of 27 – j195 Ω at 866 MHz and a read sensitivity of -18 dBm.

B. Finger Phantom

The simulated finger phantom was an 80 mm long four-layer cylindrical human tissue model as shown in Fig. 3 (b), with the parameters given in Table I. The tag under test was mounted centrally on this model for the initial simulations, then mounted 3 mm from the base of the finger above the hand section of the second hand-phantom, Fig. 3 (c). The phantom hand model was a four-layer 80 mm × 30 mm rectangular section of skin, fat, muscle and bone of thicknesses 2, 4, 3, and 5 mm respectively.

TABLE I
MATERIAL PROPERTIES AND THEIR RADII

Material	ε_r	σ (S/m)	Outer Radius (mm)
Skin	41	0.9	10.5
Fat	11.3	0.11	9
Muscle	66	0.71	na
Tendon	45.6	0.79	6.5
Bone	20.6	0.33	5
Foam substrate	1.05	< 0.0002	11/11.5
Paper substrate	2.3	0.06	10.6

C. CST Computer Simulations

Initial simulations omitted both the RFID device and tuning capacitor. With a port placed at the tuning capacitor position, an S_{11} sweep obtained port inductance for the three considered loops. Starting from the smallest diameter these were 32 nH, 45 nH and 48 nH respectively, resulting in tuning capacitor values of 1.05 pF, 0.74 pF and 0.7 pF for a center frequency of 866 MHz. Adding the equivalent impedance of the RFID port and initial C_{Tune} values, an iterative process was employed to adjust C_{Tune} and the gamma match tap point for best return loss for the three ring sizes. Radiation pattern plots were simulated, and each ring radiation efficiency was obtained for both phantom models. The results are tabulated in Table II and radiation patterns are shown in Fig. 5 where the beam direction is in the plane of the ring, and is biased along the axis of the feed which is common in small antennas. The radiation becomes directional for the three finger case with the main beam direction from the feed point.

IV. Practical Measurements and Results

A. Ring Construction and Measurements

The test samples were constructed from self-adhesive copper foil. Immersing the foam substrate in hot water increased its pliability and enabled it to be formed around the finger without damage, before being left to dry. 80 gsm office paper was used as the tuning capacitor dielectric. For a 5 mm wide conductor this results in end foil overlaps of 5.2 mm^2, 3.1 mm^2 and 2.9 mm^2 for the three capacitor values of 1.05 pF, 0.62 pF and 0.59 pF. These overlaps were left slightly oversize to allow for trimming/tuning. Fig. 6 shows a simulation plot of capacitance against plate area for the design.

TABLE II
Simulation Results

Ring Diameter (mm)	Gamma Match Tap Point*	C_{tune} (pF)	Return Loss 866 MHz (dB)	-10dB Bandwidth (MHz)	Radiation Efficiency (dB)†	Realized Gain (dBi)†
21	77°	1.05	-20.1	7.9	-16/-20.2	-14.4/-18.1
22	115°	0.62	-12.1	11.4	-11.4/-16	-9.7/-14.6
23	142°	0.59	-20.8	32	-10.1/-11.6	-8.7/-12.2

*The gamma match tap point is taken clockwise from the tuning capacitor position. †Single finger/three finger phantom results.

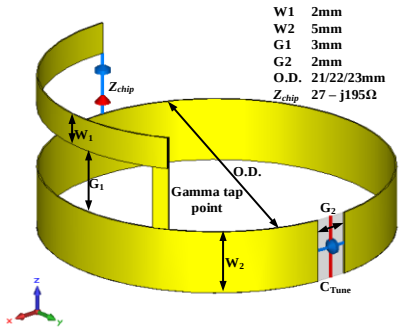

(a)

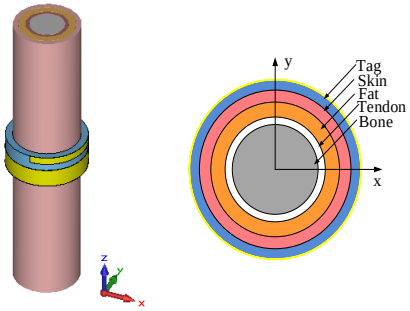

(b)

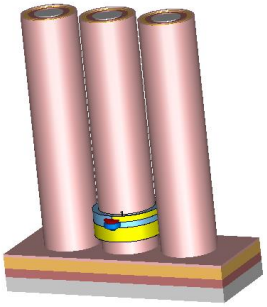

(c)

Fig. 3. (a) Ring model used for CST MWS™ simulations. (b) Finger phantom four layer cylindrical model with RFID ring antenna mounted, and (c) the three finger phantom incorporating a section of hand.

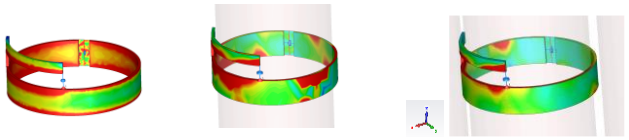

(a) (b) (c)

Fig. 4. Simulated surface current for (a) the free space model, (b) the single finger and (c) the three finger/hand phantoms.

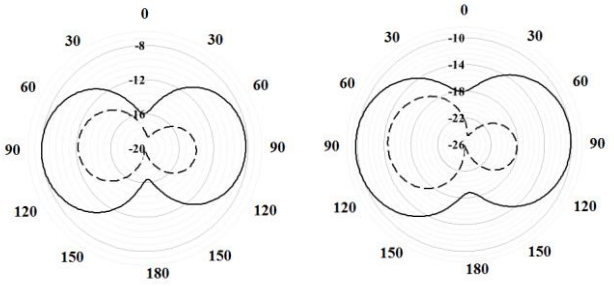

(a) (b)

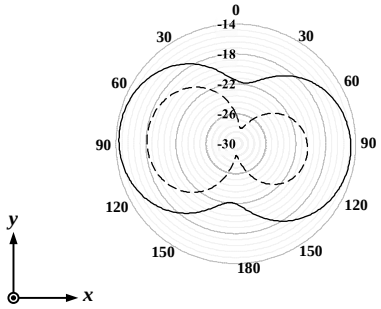

(c)

Fig. 5. Simulated radiation patterns for the three rings φ (θ = 90°), (a) 23 mm, (b) 22 mm, and (c) 21 mm for both — single finger and --- three finger/hand phantom.

With the ring on the ring finger, the resonating capacitor was trimmed to tune the loop to the European RFID band. Slight adjustment of the gamma match tap point was also carried out to optimize the the read range. The match point was found to be within a few degrees of the simulated values given in Table II.

Using a Voyantic UHF RFID measurement system, read range measurements were carried out over the three angles given in Fig. 7, where 0° relates to the loop feed point facing the reader, 90° is in the null of the loop and 180° has the tuning capacitor facing the reader. The hand maintained the same neutral relaxed position for all 3 measurements. The results are shown in Fig. 9.

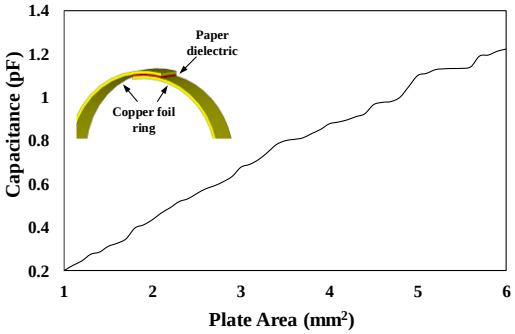

Fig. 6. Simulated capacitance against plate area for the design. Realization of the overlapping parallel plate capacitor shown inset.

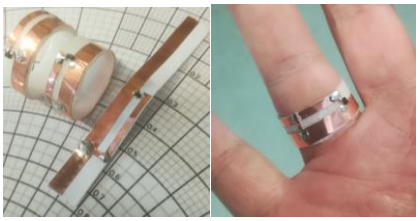

(a) (b)

Fig. 7. (a) The three constructed prototype rings, (b) the 22 mm version being worn.

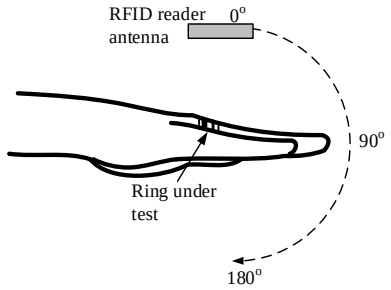

Fig. 8. RFID reader illumination angles for the practical measurements.

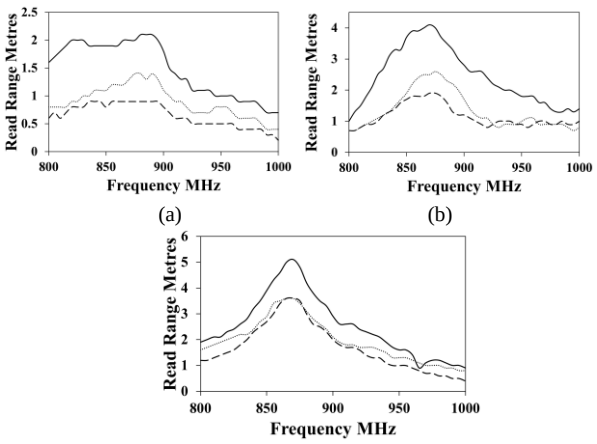

(a) (b)

(c)

Fig. 9. Voyantic read-range results for the three rings, (a) 21 mm, (b) 22 mm and (c) 23 mm at illumination angles of — 0°, --- 90°, ···· 180°.

B. *Discussion of Results*

From the measured results shown in Fig. 8 read ranges of 5.1, 4.1 and 2 m were achieved at 866 MHz for the three ring designs, resulting in realized gains of -6, -7.8 and -13.8 dB. This is an improvement compared to simulation and can be attributed to variations between the phantom model and actual test subject. Also, the simulation phantoms included identical size parallel cylinders representing the fingers at a fixed spacing of 3 mm, whereas in a relaxed hand position the fingers naturally splay outwards giving a greater distance between the tag and adjacent fingers. Moving the fingers closer together results in a downward shift in the tag center frequency though it remains in band. It is evident that with thinner substrates closer to the skin the ring efficiency and read range is reduced. The practical measurements also show a significant broadening of bandwidth (lower Q) for decreasing values of substrate height, particularly for the on-paper design. However, a 2 m read range for a small low-profile on-body tag is considered a very useable distance, whilst 5.1 m is available for the 2 mm thick substrate version which would cover most rooms. In their current format the rings would be considered a single region design but they could be tuned for other UHF RFID regions i.e. North America or Asia by modification of the tuning capacitor value. The practical measurements exhibit directivity in agreement with the three finger phantom simulations with maximum radiation being at the feed-point for all three designs. This could be a consideration when mounting the rings.

V. Conclusions and Future Work

Three prototype finger ring tags were designed and fabricated targeted at the European RFID band of 866 MHz. Read ranges exceeding 2 m were achieved despite the compact tag size and their proximity to the lossy human body. Currently only an adult male ring finger has been used for testing of the designs, and further work is to be carried out on other digits, including toes. It is also considered that the design could be adapted for use on the small limbs of premature babies or potentially on animals for stock control or wildlife monitoring. At the dimensions considered (0.18-0.2λ) they exhibit maximum radiation in the plane of the loop and only at lengths of ≥ 0.3λ would a broadside radiation pattern occur similar to that of a large loop. Employing a more sophisticated sensor type RFID chip would enable additional functionality to be added, for instance for patient health monitoring. The design would lend itself to printed manufacture using conductive inks and this is under further investigation.

VI. Acknowledgement

This research was supported by EPSRC project EP/P027075/1

References

[1] Yeo, W.-H., Y.-S. Kim, et al. (2013). "Multifunctional Epidermal Electronics Printed Directly Onto the Skin." Advanced Materials 25(20): 2773-2778.

[2] Kim, D.-H., N. Lu, et al. (2011). "Epidermal Electronics." Science 333(6044): 838-843.

[3] Madhvapathy, S. R., Y. Ma, et al. (2018). "Epidermal Thermal Depth Sensors: Epidermal Electronic Systems for Measuring the Thermal

Properties of Human Skin at Depths of up to Several Millimeters (Adv. Funct. Mater. 34/2018)." Advanced Functional Materials 28(34):

[4] P. S. Taylor and J. C. Batchelor, "Small Epidermal UHF RFID Loop Antenna for Passive Oral Cavity Control Applications and Patient Health Monitoring," *2018 IEEE International Symposium on Antennas and Propagation & USNC/URSI National Radio Science Meeting*, Boston, MA, 2018, pp. 687-688.

[5] D. O. Oyeka *et al*., "Inkjet printed epidermal RFID tags," *The 8th European Conference on Antennas and Propagation (EuCAP 2014)*, The Hague, 2014, pp.1403-1406.

[6] S. Milici, S. Amendola, A. Bianco and G. Marrocco, "Epidermal RFID passive sensor for body temperature measurements," *2014 IEEE RFID Technology and Applications Conference (RFID-TA)*, Tampere, 2014, pp. 140-144.

[7] O. O. Rakibet, C. V. Rumens, J. C. Batchelor and S. J. Holder, "Epidermal Passive RFID Strain Sensor for Assisted Technologies," in *IEEE Antennas and Wireless Propagation Letters*, vol. 13, pp. 814-817, 2014.

[8] S. Amendola, S. Milici, G. Marrocco and C. OCChiuzzi, "On-skin tunable RFID loop tag for epidermal applications," *2015 IEEE International Symposium on Antennas and Propagation & USNC/URSI National Radio Science Meeting*, Vancouver, BC, 2015, pp. 202-203.

[9] M. A. Ziai and J. C. Batchelor, "Supply chain integrity tilt sensing RFID tag," *2017 IEEE MTT-S International Microwave Workshop Series on Advanced Materials and Processes for RF and THz Applications (IMWS-AMP)*, Pavia, 2017, pp.1-3.

[10] D. O. Oyeka, M. A. Ziai and J. C. Batchelor, "RFID sticking plasters," *2012 Loughborough Antennas & Propagation Conference (LAPC)*, Loughborough, 2012, pp.1-4.

[11] D. P. Rose *et al*., "Adhesive RFID Sensor Patch for Monitoring of Sweat Electrolytes," in *IEEE Transactions on Biomedical Engineering*, vol. 62, no. 6, pp. 1457-1465, June 2015.

[12] A. Rashee, E. Iranmanes, W. Li, X. Fen, A. S. Andrenk and K. Wan, "Experimental study of human body effect on temperature sensor integrated RFID tag," *2017 IEEE International Conference on RFID Technology & Application (RFID-TA)*, Warsaw, 2017, pp. 243-247.

[13] T. Kellomaki, "On-Body Performance of a Wearable Single-Layer RFID Tag," in *IEEE Antennas and Wireless Propagation Letters*, vol. 11, pp. 73-76, 2012.

[14] B. Waris, L. Ukkonen, J. Virkki and T. Björninen, "Wearable passive UHF RFID tag based on a split ring antenna," *2017 IEEE Radio and Wireless Symposium (RWS)*, Phoenix, AZ, 2017, pp. 55-58.

[15] T. Björninen, J. Virkki and L. Ukkonen, "Small square-shaped slot antenna for wearable passive UHF RFID tags," *2017 International Applied Computational Electromagnetics Society Symposium (ACES)*, Suzhou, 2017, pp. 1-2.

[16] S. Manzari, S. Pettinari and G. Marrocco, "Miniaturised wearable UHF-RFID tag with tuning capability," in *Electronics Letters*, vol. 48, no. 21, pp. 1325-1326, 11 October 2012.

[17] Svanda, M & Milan, Polivka. (2014). Small-size wearable high-efficiency TAG antenna for UHF RFID of people. International Journal of Antennas and Propagation. 2014. 1-5.

[18] M. J. Underhill and M. J. Blewett, "Magnetic loop or small folded dipole?" *Seventh International Conference on HF Radio Systems and Techniques*, Nottingham, UK, 1997, pp. 216-225.

[19] A. Boswell, "Loop antennas in the 3-30 MHz band," *2000 Eighth International Conference on HF Radio Systems and Techniques*, Guildford, UK, 2000, pp. 33-36.

[20] D.B. Miron, *Small Antenna Design*, Newnes Publications, ISBN 978-0-7506-7861-2 pp 33-34.

[21] B. A. Austin, A. Boswell and M. A. Perks, "Loss Mechanisms in the Electrically Small Loop Antenna [Antenna Designer's Notebook]," in *IEEE Antennas and Propagation Magazine*, vol. 56, no. 4, pp. 142-147, Aug. 2014.

[22] J. S. Belrose, "Performance Analysis of Small Tuned Transmitting Loop Antennas Evaluated by Experiment and Simulation [Antenna Designer's Notebook]," in *IEEE Antennas and Propagation Magazine*, vol. 49, no. 3, pp. 128-132, June 2007.